

# DFT Study on Isomerization and Decomposition of Cuprous Dialkyldithiophosphate and Its Reaction with Alkylperoxy Radical

Yi Luo, Satoshi Maeda, and Koichi Ohno\*

Department of Chemistry, Graduate School of Science, Tohoku University, Aramaki, Aoba-ku, Sendai 980-8578, Japan

Received: February 22, 2008; Revised Manuscript Received: April 4, 2008

The cuprous dialkyldithiophosphate [(RO)<sub>2</sub>PS<sub>2</sub>Cu, CuDDP] as an antioxidant has been industrially used in lubricating oil. In this paper, for the first time, a computational study has been carried out for CuDDP. The scaled hypersphere search method has been used to explore the isomerization and decomposition pathways of (HO)<sub>2</sub>PS<sub>2</sub>Cu, a model compound of CuDDP, and its reaction with CH<sub>3</sub>OO• radical. The calculations were performed at the B3LYP level of theory. The results show that the most stable structure of (HO)<sub>2</sub>PS<sub>2</sub>Cu has pseudo-C<sub>2v</sub> symmetry and a four-membered ring constructed by P, Cu, and two S atoms. The bond-rearrangement isomerization leading to a (H)O-bridging structure is kinetically feasible. Three dissociation channels have been found for (HO)<sub>2</sub>PS<sub>2</sub>Cu, which require high energy (>60 kcal/mol) under the investigated condition. The reaction of (HO)<sub>2</sub>PS<sub>2</sub>Cu with CH<sub>3</sub>OO• includes bond-rearrangement isomerization and the decomposition of CH<sub>3</sub>OO• moiety. The (HO)<sub>2</sub>PS<sub>2</sub>Cu-assisted CH<sub>3</sub>OO• decomposition occurs via its O—O bond cleavage or the C—O bond dissociation. The former decomposition manner has been computed to be preferable over the latter at low temperature, but calculations suggested for the latter decomposition manner at higher temperature. Such a decomposition reaction, which is endothermic but possible, may be related to the antioxidation process of CuDDP.

## Introduction

Lubricating oils in crankcase automotive engines are known to undergo oxidative degradation leading to products believed to be responsible for sludge deposits in used oils. Oil deterioration results in a loss of lubrication, with the signals shown by the appearance of sludge. Efforts aimed at reducing sludgy formation may extend the life span of the lubricant and prevent failure in service. Utilizing of additives, such as antioxidant and antiwear agent, is a common strategy to inhibit oil oxidation and avoid friction on the surface of engine parts and therefore reduce the formation of sludge.<sup>1</sup> Like other organic substrates, the autoxidation of lubricants follows free-radical reaction mechanism<sup>2</sup> (Scheme 1). As shown in Scheme 1, the reactions (1) and (2) form a chain reaction. To prevent such oil autoxidation process, antioxidants are often used to scavenge the alkylperoxy radical and in turn to terminate the chain reaction. Dialkyldithiophosphate transition-metal salts, such as cuprous dialkyldithiophosphate (CuDDP, see Chart 1a), can serve as an effective radical scavenger in lubricating oil. As an antioxidation additive in lubricating oil, the CuDDP has been industrially applied for a long time. Since it was discovered more than 50 years ago,<sup>3</sup> numerous experimental studies<sup>4–7</sup> have been done in laboratory with the aim of synthesis and usage of such an additive, most of which were reported as patents.<sup>5–7</sup> It is known that the CuDDP is an efficient antioxidant by scavenging the alkylperoxy radical, especially at high temperature. One of the authors previously synthesized the CuDDP and tested its antioxidation properties.<sup>4b</sup> The experimental work on the reaction of organic peroxy radicals with Cu(I) species has also been reported previously.<sup>8</sup> The decomposition reaction of alkylperoxy radical (ROO•) would occur via either its O—O

## SCHEME 1: Autoxidation of Lubricating Oil

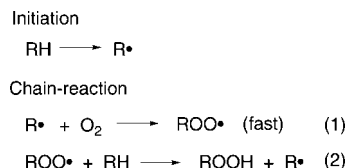
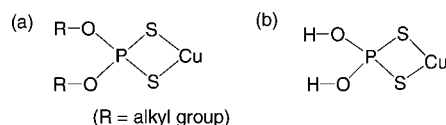


## CHART 1: (a) Schematic Representation of CuDDP and (b) Model Compound of CuDDP



bond cleavage or the R—O (C—O) bond dissociation. Obviously, detailed knowledge about how these additives behave is of great importance for their development and usage. In spite of wide experimental studies,<sup>4–7</sup> however, the mechanistic knowledge about the isomerization and decomposition of CuDDP as well as its reaction with alkylperoxy radical is very limited. For example, the isomerization potential energy surface (PES) of CuDDP and the CuDDP-assisted decomposition manner of alkylperoxy radical remain unknown. Moreover, the CuDDP has not been structurally characterized as far as we are aware, although its multinuclear cluster and its derivatives bearing ancillary ligand have been isolated and well defined.<sup>9–13</sup> A computational optimization of the geometry of CuDDP can give structural information and would therefore be helpful for future study of such compound.

The chemical behaviors of zinc(II) analogue, zinc(II) dialkyldithiophosphate [((RO)<sub>2</sub>PS<sub>2</sub>)<sub>2</sub>Zn, ZnDDP], which mainly serves as an antiwear agent in lubricating oil, have been recently

\* Corresponding author. E-mail: ohnok@qpcrkk.chem.tohoku.ac.jp.

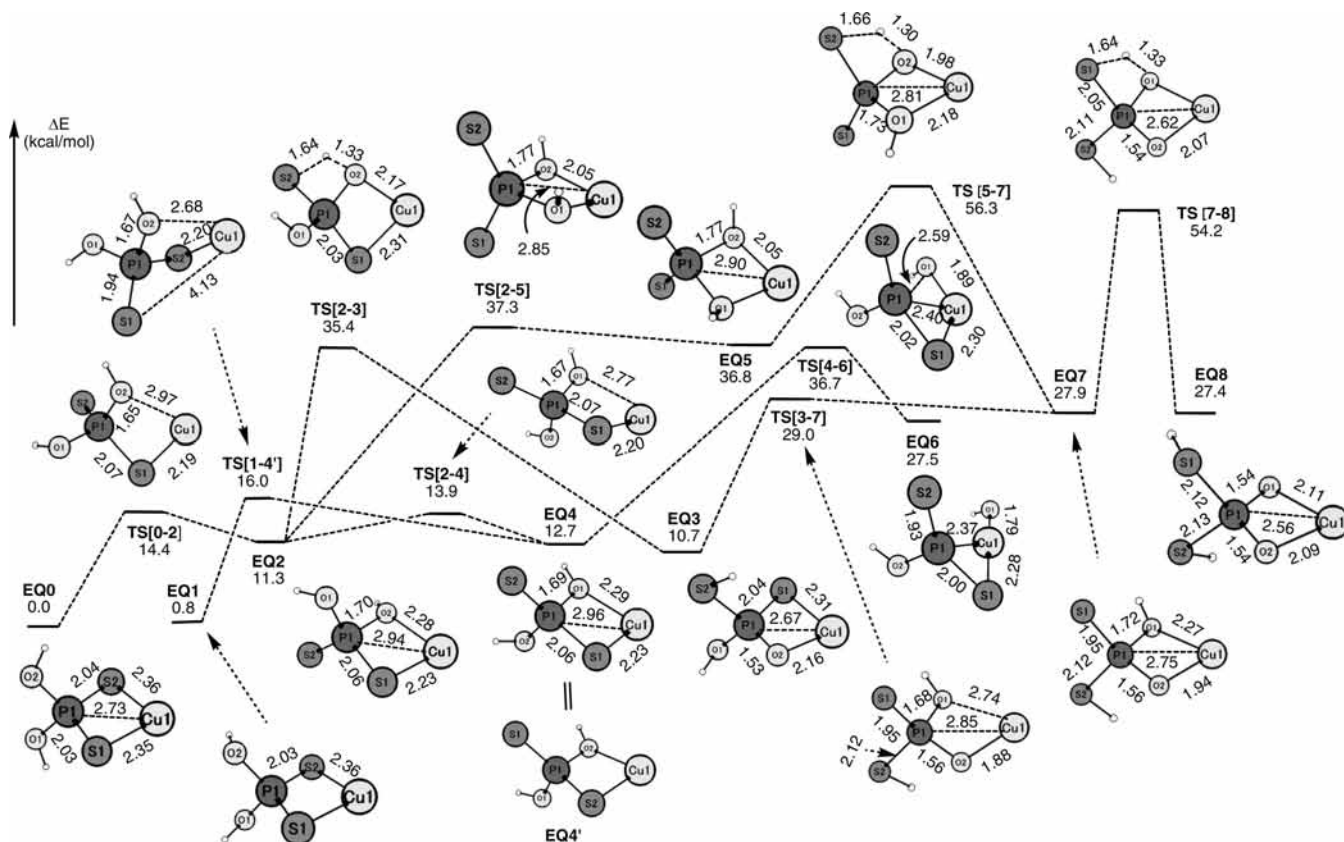


**Figure 1.** Stationary points (bond lengths in Å) together with their relative energies (kcal/mol) for the isomerization of  $(\text{OH})_2\text{PS}_2\text{Cu}$ . The energies computed at the level B3LYP/BSII//B3LYP/BSI are relative to **EQ0**.

computationally investigated by Woo et al.<sup>14</sup> Their static and dynamic computations revealed the decomposition mechanism of ZnDDP and the formation process of protecting film on the surface of engine parts. Their static calculations also showed that the current DFT method is capable of dealing with such system. In their works, the temperature effect on the related reactions was also investigated, and the average operating temperature on the surface of engine parts was considered to be 500K. As for the CuDDP, the isomerization and decomposition process as well as antioxidation mechanism, which are difficult to experimentally investigate in detail, are yet to be fully understood. To the best of our knowledge, however, no computational work on CuDDP was reported to date. This is possibly due to the fact that it is hard to model the reaction process. That is, it is not easy to guess the reaction intermediates and products, especially for the isomerization and decomposition reaction. In this connection, our group has successfully developed the scaled hypersphere search (SHS) method, which enables one to globally explore reaction pathways on the PES by detecting anharmonic downward distortions (ADD) as a symptom of chemical reaction.<sup>15</sup> This method may automatically search for the reaction routes without any initial guess of intermediates or TSs. The SHS method has been successfully used to investigate unimolecular chemical reactions on the basis of global reaction route mapping.<sup>16</sup> For its application to larger systems, the large-ADD (LADD) technique has been introduced to the SHS method, and the search for a reaction route can be executed at the low energy region of PES. Such a technique has been applied to molecular clusters.<sup>17</sup> The combination of ONIOM approach<sup>18</sup> and the LADD technique in the SHS method has been also recently achieved and applied to BINAP system.<sup>19</sup> In this work, the LADD technique in the SHS method

has been utilized to study the isomerization and decomposition of CuDDP and its reaction with  $\text{CH}_3\text{OO}\cdot$  radical.

### Computational Method

The SHS method is an uphill-walking technique to automatically explore reaction pathway from a given equilibrium structure (EQ). To effectively detect the ADD, a given EQ-centered hypersphere surface is introduced in the SHS technique. Such a hypersphere surface is expanded by the scaled normal coordinates  $q_i$ , which can be defined by normal coordinates  $Q_i$  and the respective eigenvalues  $\lambda_i$ , with  $q_i = \lambda_i^{1/2} Q_i$ . During the reaction pathway following the scaled hypersphere surface, the conventional optimization scheme and downhill-walking technique may be utilized. For each transition state (TS) found, the intrinsic reaction coordinate (IRC) was automatically executed to confirm the connection to its terminus. Such a pathway tracking may lead to TSs, dissociation channels, and new EQs. After the reaction pathways are traced for all of EQs via a one-after-another manner, the global PES may be therefore figured out.

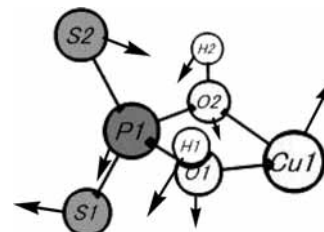
A model compound  $(\text{HO})_2\text{PS}_2\text{Cu}$  (Chart 1b) of  $(\text{RO})_2\text{PS}_2\text{Cu}$  was used in the pathway explorations. However, the effect of alkyl R group has been also investigated for some reactions. All of the calculations were performed at the B3LYP level of theory.<sup>20</sup> The LanL2DZ basis set and associated pseudopotential<sup>21</sup> was used for the Cu atom. Considering a radical species involved in the current system, the 6-31+G\*\* basis set<sup>22</sup> including diffuse function was used for C, H, O, S, and P atoms. Such basis set combination is represented here by BSI. It is found that an augmentation of the  $f$  polarization function (exponent of 3.525)<sup>23</sup> for Cu atom does not significantly alter the geometry of  $(\text{HO})_2\text{PS}_2\text{Cu}$  (variation of  $\sim 0.001$  Å in bond

length, see Supporting Information). The geometry optimization with all-electron basis sets (the 6-311+G\* basis set<sup>24</sup> for the Cu atoms and the 6-31+G\*\* for the remaining ones) has been performed also for (HO)<sub>2</sub>PS<sub>2</sub>Cu. The result shows small changes in bond lengths (less than 0.05 Å, see Supporting Information). Therefore, the geometry optimizations were carried out at the B3LYP/BSI level to save computational time. The subsequent analytic frequency calculations were performed for each stationary point to verify the minima and TSs and to get the thermodynamic data. The IRCs were followed during the SHS calculations. To obtain more accurate energy, single-point calculation with a larger basis set (BSII) was performed for the B3LYP/BSI geometries. In the BSII, the 6-311+G\* basis set<sup>24</sup> containing the *f* polarization function was used for the Cu atom and the 6-311+G\*\* basis set<sup>25</sup> for the remaining atoms. The free energy reported in this study was computed at B3LYP/BSII/B3LYP/BSI, including the free-energy contribution from the B3LYP/BSI calculations, if not stated otherwise. The stabilities of wave functions were tested. Except for the SHS procedures, all of the calculations were carried out by utilizing the Gaussian 03 program.<sup>26</sup>

## Results and Discussion

By using the SHS method, the reaction PES was explored in the gas phase. However, the solvent effect was estimated for some reactions. Considering that the average operating temperature on the surface of engine parts is generally considered to be 500 K, the temperature (300–700 K) effect on the free energy was also investigated. The computed gas-phase energy profile of (HO)<sub>2</sub>PS<sub>2</sub>Cu isomerization is shown in Figure 1, where the important interatomic distances are also included. The stationary points shown in this figure were located at the low-energy region of the PES by using the SHS method. As seen in Figure 1, the most stable structure **EQ0** has a four-membered ring constructed by the P1, S1, Cu1, and S2 atoms. The Cu1–S1 and Cu1–S2 bond lengths are almost equal, suggesting nearly equal bindings between the Cu and two S atoms. The same is true for the P1–S1 and P1–S2 bonds. The O, P, S, and Cu atoms in the **EQ0** constructed a pseudo-*C<sub>2v</sub>* geometry. These structural characters are similar to its zinc analogous [(RO)<sub>2</sub>PS<sub>2</sub>]<sub>2</sub>Zn and to one of its derivatives, which was experimentally well defined.<sup>9</sup> The **EQ0** may go through a TS, **TS[0–2]**, leading to **EQ2**. In the **EQ2**, an OH group geometrically replaced the S2 atom to bind both P1 and Cu1 atoms. Such structural changes made the P1...Cu1 distance longer (2.94 Å) in comparison with that of **EQ0** (2.73 Å). The **EQ2** is unstable by 11.3 kcal/mol compared to the **EQ0**. Such destabilization may be partly caused by the distortion of the four-membered ring (P1S1Cu1O2) in the **EQ2**. An analysis of the imaginary mode of the **TS[0–2]** indicates a rotation of (OH)<sub>2</sub>(S2)P1 group around the P1–S1 bond axis. There is an energy barrier of 14.4 kcal/mol for the conversion of **EQ0** to **EQ2**. The (OH)<sub>2</sub>(S2)P1 group in the **EQ2** continues to rotate around the P1–S1 bond axis to give **EQ4** via a **TS[2–4]**. This transformation is quite easy because there is a very small energy barrier (2.6 kcal/mol) to separate the **TS[2–4]** from **EQ2**. It is noticed that the transformation from the **EQ0** to **EQ4** is endothermic by 12.7 kcal/mol. Such an endothermic character and a lower energy barriers (1–3 kcal/mol) for the reverse process (from the **EQ4** to **EQ0**) suggest that the transformation from the **EQ0** to **EQ2** and further to **EQ4** is not highly favored, both thermodynamically and kinetically. This result indicates that the **EQ0** could be the predominant component under the investigated condition.

**CHART 2: Displacement Vectors of the Imaginary Mode (*i*35 cm<sup>-1</sup>) of TS[2-5]**



As the result of the search for isomers by the SHS method, an isomeric structure **EQ1** has been found also. The **EQ1** is less stable by 0.8 kcal/mol compared to the **EQ0**. The two isomers (**EQ0** and **EQ1**) have similar geometrical structures, but the relative orientations of their OH groups are different. Similar to the transformation from the **EQ0** to **EQ2**, the (OH)<sub>2</sub>(S1)P1 group in the **EQ1** may also rotate around the P1–S2 bond axis to yield **EQ4'** via a TS **TS[1–4']**. This transformation needs an energy barrier of 15.2 kcal/mol and is endothermic by 11.9 kcal/mol relevant to **EQ1**. The **EQ4'** is structurally and hence energetically identical to the **EQ4**. In the **EQ2**, the H atom of O2H group can transfer to S2 atom via a TS, **TS[2–3]**, leading to **EQ3**. With this transformation, the P...Cu contact decreased from 2.94 Å in the **EQ2** to 2.67 Å in the **EQ3**. Such structure change made the **EQ3** slightly stable by 0.6 kcal/mol compared to the **EQ2**. A moderate energy barrier (24.1 kcal/mol) is necessary for such a hydrogen transfer process. This suggests that the transfer of alkyl group (R) from an O to S atom is a possible isomerization manner of CuDDP. Such a transfer event was suggested for ZnDDP previously.<sup>14</sup> The **EQ2** may also lead to **EQ5** with a four-membered ring motif (P1O1Cu1O2) involving two O atoms. This transformation needs to overcome a TS, **TS[2–5]**, with an energy barrier of 26.0 kcal/mol. Although such an energy barrier is similar to that (24.1 kcal/mol) for **TS[2–3]** leading to the **EQ3**, the **EQ5** is significantly higher in energy than the **EQ3**. This suggests that the conversion of **EQ2** to **EQ5** is thermodynamically unfavorable compared to the transformation from the **EQ2** to **EQ3**. It is noteworthy that an analysis of imaginary mode of **TS[2–5]** shows an out-of-plane bending vibration (see Chart 2 for the displacement vector) but no rotation of an organic group like that for **TS[0–2]**, **TS[1–4']**, and **TS[2–4]**. The small imaginary frequency value (*i*35 cm<sup>-1</sup>) and the flat PES region around the **TS[2–5]** and **EQ5** suggest that the conversion of the **EQ2** to **EQ5** is not desirable. There is a moderate energy barrier (24.0 kcal/mol) for the conversion of the **EQ4** to **EQ6** via **TS[4–6]**, during which the cleavage of P1–O1 bond and the formation of P1–Cu1 bond are concerted. However, this transformation is endothermic by 14.8 kcal/mol relevant to the **EQ4**, suggesting that the formation of **EQ6** is thermodynamically undesirable. It is also found that the conversion of **EQ3** to the (HS)<sub>2</sub>PO<sub>2</sub>Cu species (**EQ8**) occurred via organic group rotation (leading to the **EQ7**) and hydrogen transfer, like the transformation from the **EQ0** to **EQ3**. The TS, **TS[7–8]**, leading to the **EQ8** has a rather high energy (54.2 kcal/mol relative to the **EQ0**), and the **EQ8** is less stable by 16.7 kcal/mol compared to the **EQ3**. This suggests that the formation of the **EQ8** is unfavorable compared to that of **EQ3**. There is another pathway leading to the **EQ7**, which goes through the **TS[5–7]**, having a high energy (56.3 kcal/mol relative to the **EQ0**), and is unfavorable compared to the route from the **EQ3** to **EQ7**.

As seen in Figure 1, the transformations among **EQ0**, **EQ1**, **EQ2**, and **EQ4** are more preferable in comparison with other

**TABLE 1: Interatomic Distances (Å) and Relative Energies (kcal/mol) Computed at the B3LYP and MP2 Levels<sup>a</sup>**

	EQ0	TS[0–2]	EQ2
P1–S1	2.03 (2.00)	2.07 (2.03)	2.06 (2.02)
P1–S2	2.04 (2.01)	1.96 (1.95)	1.95 (1.93)
P1···Cu1	2.73 (2.75)	3.08 (2.83)	2.94 (2.88)
S1–Cu1	2.35 (2.36)	2.19 (2.25)	2.23 (2.28)
S2–Cu1	2.36 (2.37)		
P1–O2	1.62 (1.62)	1.65 (1.66)	1.70 (1.71)
O2···Cu1		2.97 (2.74)	2.28 (2.20)
Relative Energy	0.0 (0.0)	14.4 (17.9)	11.3 (15.2)

<sup>a</sup> BSI was used for geometry optimization, and BSII was used for energy calculation on the optimized geometry. The data with and without parentheses are computed at the B3LYP and MP2 levels, respectively.

pathways. The **EQ0** may have significant predominance over other isomers with respect to the computed energy. This led us to use the structure of **EQ0** for (HO)<sub>2</sub>PS<sub>2</sub>Cu to model the reaction of (HO)<sub>2</sub>PS<sub>2</sub>Cu with CH<sub>3</sub>OO• species (vide info).

It is computationally expensive to combine the SHS and higher computational level, such as MP2,<sup>27</sup> to explore the PES of such system. However, we have additionally made MP2 calculations for some important stationary points, **EQ0**, **TS[0–2]**, and **EQ2** in Figure 1, to compare with the B3LYP results (Table 1). It is found that the variations in the interatomic distances are less than 0.08 Å except for the P1···Cu1 and O2···Cu1 contacts (variations of 0.25 and 0.23 Å, respectively) in the **TS[0–2]** (Table 1). Such larger variations in the TS are possibly due to the fact that B3LYP could not estimate better the weak interaction (P1···Cu1 and O2···Cu1). As seen from Table 1, the B3LYP underestimated the relative energies by less than 4.0 kcal/mol compared to the MP2 method. These insignificant discrepancies may be used for estimating the methodological errors but did not alter the conclusion drawn here. Therefore, we could not further perform MP2 calculations for all stationary points for the sake of computational time.

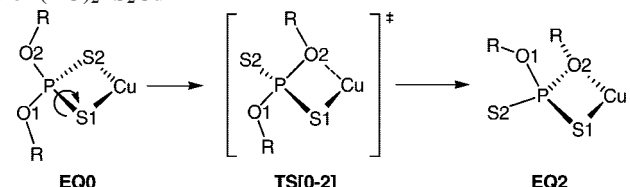
To see whether the R substituent of CuDDP has significant effects on the isomerization energy, seven alkyl substituents covering C<sub>3</sub>, C<sub>5</sub>, and C<sub>8</sub> alkyl chains were selected as R groups of (RO)<sub>2</sub>PS<sub>2</sub>Cu to computationally investigate the transformation (Table 2), such as that from **EQ0** to **EQ2**, which exemplifies the bond-rearrangement isomerization of (HO)<sub>2</sub>PS<sub>2</sub>Cu. The CuDDP containing C<sub>8</sub> alkyl group is typically used in engine oil, possibly because of its better oil solubility and thermal stability. The energies reported in Table 2 are obtained from the B3LYP/BSI calculations. Considering that the energies for the (HO)<sub>2</sub>PS<sub>2</sub>Cu isomerization, such as the transformation from the **EQ0** to **EQ2** (Table 2 and Figure 1) is not significantly dependent on the computational levels, B3LYP/BSI and B3LYP/BSII//B3LYP/BSI, we could not calculate the CuDDP having alkyl substituents at the B3LYP/BSII level because more computational time was required for bulky R groups. As seen from Table 2, in the case of CuDDP having alkyl substituents, both energy barrier and reaction energy are slightly higher than those for the (HO)<sub>2</sub>PS<sub>2</sub>Cu model compound. However, the variations are only about 2 kcal/mol. This result suggests that the substituents have no significant effects on the energies in the isomerization process investigated.

We also further investigated the temperature effect on the relative free energies of the stationary points involved in the isomerization of (HO)<sub>2</sub>PS<sub>2</sub>Cu (Figure 1). The results are shown in Table 3. The temperature range of 300–700 K is chosen here because the average temperature of engine surface is

generally considered to be ~500 K. As seen from Table 3, with the temperature change, the free energies of EQs and TSs relative to **EQ0** varied by 0.3–2.5 kcal/mol. A close look at the data in Table 3 indicates that the relative energies of the EQs gradually decrease with increasing temperature. But the relative energies of TSs increase with temperature. Although the temperature-dependent variations in these relative energies are small, such trends are clear. This result may suggest that the entropies of the TSs are slightly different from those of EQs.

During the reaction-pathway exploration, the dissociation channels of CuDDP have also been discovered by the SHS method. Table 4 shows three dissociation channels and the associated dissociation free energies at selected temperatures. The choice of temperatures in Table 4 is also based on the average working temperature (500 K) of the engine surface. As seen from this table, the decomplexation of (HO)<sub>2</sub>PS<sub>2</sub>Cu, which leads to (HO)<sub>2</sub>PS<sub>2</sub><sup>−</sup> and Cu<sup>+</sup> ions, requires a higher energy (>178 kcal/mol) in comparison with the other two dissociation channels (63–82 kcal/mol) leading to radical species. The latter two channels may be relevant to the dissociation of the alkyl (−R) and the alkoxy (−OR) groups of CuDDP. This result suggests that the decomplexation of CuDDP is unlikely to occur under the investigated temperatures. With the temperature increasing, the dissociation energy significantly decreases for the channel leading to (HO)(•P)S<sub>2</sub>Cu and •OH but slightly increases for the other two channels leading to atomic species (Cu<sup>+</sup> or •H). This is easy to understand because the dissociated species are quite entropically different. Such result suggests that the dissociation reaction leading to •OH radical gets easier at higher temperature. However, even at high temperature, such as 700 K, the dissociation energy (Table 4) is significantly higher in comparison with the isomerization energy barrier (Table 3 and Figure 1), suggesting that the isomerization of (HO)<sub>2</sub>PS<sub>2</sub>Cu is preferable over its decomposition.

In addition to its isomerization and decomposition, CuDDP as a radical scavenger could be involved in other complex chemical reaction in the lubricating oil. In this sense, the reaction of (HO)<sub>2</sub>PS<sub>2</sub>Cu with CH<sub>3</sub>OO•, as a model reaction, was also investigated. Figure 2 shows some reaction pathways discovered by using the SHS method. Such processes include bond-rearrangement isomerization and the decomposition of alkylperoxy radical. The reaction of (HO)<sub>2</sub>PS<sub>2</sub>Cu with CH<sub>3</sub>OO• starts from their complexation. As shown in Figure 2, two coordination complexes, **EQ9** and **EQ10**, were located on the PES. With respect to the isolated reactants [(HO)<sub>2</sub>PS<sub>2</sub>Cu + CH<sub>3</sub>OO•], the formation of the **EQ10** is exothermic by 29.7 kcal/mol (Figure 2). According to the computed energy, **EQ9** is less stable by 2.3 kcal/mol compared to **EQ10**. Such minor energy difference may result from their different coordination situations. In the **EQ9**, both oxygen atoms of the CH<sub>3</sub>OO• moiety significantly coordinate to the Cu atom, as suggested by the distances of Cu1–O2 (1.89 Å) and Cu1–O1 (2.22 Å) and the Wiberg bond index (WBI) of the two bonds (0.10 for Cu1–O1 and 0.39 for Cu1–O2). Such a situation suggests that the CH<sub>3</sub>OO• coordinates to the metal center in a (μ, η<sup>2</sup>) fashion via its two O atoms. On the other hand, the longer distances (2.76 Å) and smaller WBI (0.05) of Cu1···O1 contact in the **EQ10** suggests a very weak (or nearly no) interaction between Cu1 and O1 atoms in this EQ. The Cu1–O2 distance of 1.87 Å and the WBI of 0.29 for the Cu1–O2 bond suggest the Cu1–O2 bonding in the **EQ10**. In this sense, we may tentatively assign the **EQ10** as a (μ, η<sup>1</sup>) complex. The slightly lower stability of the **EQ9** may result from the strained triangle (Cu1O2O1) coordination

**TABLE 2: Energy Barrier and Reaction Energy<sup>a</sup> for a Transformation such as That From EQ0 to EQ2 Via TS[0-2] with Respect to Various R Substituents of (RO)<sub>2</sub>PS<sub>2</sub>Cu**


R	energy barrier <sup>b</sup>	reaction energy <sup>c</sup>
H	13.0 (12.6) [13.3]	11.4 (11.5) [10.7]
propyl [-CH <sub>2</sub> CH <sub>2</sub> CH <sub>3</sub> ]	15.3 (14.9) [15.6]	12.4 (12.5) [11.8]
iso-propyl [-CH(CH <sub>3</sub> )CH <sub>3</sub> ]	15.3 (14.9) [15.1]	12.5 (12.6) [11.4]
pentyl [-CH <sub>2</sub> (CH <sub>2</sub> ) <sub>3</sub> CH <sub>3</sub> ]	15.2 (14.9) [15.3]	13.2 (13.2) [13.0]
isopentyl [-CH <sub>2</sub> CH(CH <sub>3</sub> )CH <sub>2</sub> CH <sub>3</sub> ]	15.2 (14.8) [15.6]	13.3 (13.4) [12.0]
octyl [-CH <sub>2</sub> (CH <sub>2</sub> ) <sub>6</sub> CH <sub>3</sub> ]	15.1 (14.8) [14.3]	13.1 (13.1) [12.5]
iso-octyl [-CH <sub>2</sub> CH(CH <sub>3</sub> )CH <sub>2</sub> C(CH <sub>3</sub> ) <sub>3</sub> ]	15.0 (14.8) [15.5]	13.4 (13.2) [11.7]
2-methyl-octyl [-CH <sub>2</sub> CH(CH <sub>3</sub> )(CH <sub>2</sub> ) <sub>4</sub> CH <sub>3</sub> ]	15.2 (14.9) [15.3]	13.2 (13.3) [12.1]

<sup>a</sup> Electronic energy including zero-point energy correction, enthalpy (in parenthesis), and free energy (298 K, in bracket) are given in kcal/mol. They were computed at the level B3LYP/BSI. <sup>b</sup> Defined as  $E_{(TS[0-2])} - E_{(EQ0)}$ , where the  $E_{(TS[0-2])}$  and  $E_{(EQ0)}$  denote the energies of TS[0-2] and EQ0, respectively. <sup>c</sup> Defined as  $E_{(EQ2)} - E_{(EQ0)}$ , where the  $E_{(EQ2)}$  and  $E_{(EQ0)}$  denote the energies of EQ2 and EQ0, respectively.

**TABLE 3: Temperature Effect on the Relative Free Energies (kcal/mol) of Stationary Points Involved in the Isomerization of (OH)<sub>2</sub>PS<sub>2</sub>Cu<sup>a</sup>**

	relative free energies				
	300 K	400 K	500 K	600 K	700 K
EQ0	0.0	0.0	0.0	0.0	0.0
EQ1	1.1	1.1	1.2	1.3	1.4
EQ2	11.9	11.6	11.3	10.9	10.6
EQ3	10.4	10.2	10.1	10.0	9.8
EQ4	11.3	10.8	10.2	9.7	9.1
EQ5	36.9	36.7	36.6	36.5	36.6
EQ6	26.9	26.6	26.2	25.9	25.5
EQ7	26.0	25.9	25.8	25.7	25.6
EQ8	23.6	23.5	23.3	23.1	22.9
TS[0-2]	14.7	15.0	15.3	15.7	16.0
TS[1-4]	16.3	16.5	16.8	17.1	17.4
TS[2-3]	35.8	36.1	36.4	36.8	37.2
TS[2-4]	14.1	14.4	14.6	14.9	15.2
TS[4-6]	36.9	37.0	37.2	37.4	37.6
TS[2-5]	38.3	38.9	39.5	40.1	40.8
TS[3-7]	26.5	26.8	27.1	27.5	28.0
TS[5-7]	53.3	53.6	53.9	54.3	54.7
TS[7-8]	49.5	49.7	50.0	50.3	50.4

<sup>a</sup> The structures of stationary points (EQs and TSs) are shown in Figure 1. Energies are relative to EQ0.

**TABLE 4: Dissociation Free Energies (kcal/mol) of (OH)<sub>2</sub>PS<sub>2</sub>Cu under Various Temperatures (K)**

temperature	dissociation product		
	(HO) <sub>2</sub> PS <sub>2</sub> <sup>-</sup> + Cu <sup>+</sup>	(HO)(•O)PS <sub>2</sub> Cu + •H	HO(•P)S <sub>2</sub> Cu + •OH
300	178.3	81.0	78.7
400	179.5	81.2	74.7
500	180.8	81.5	70.8
600	182.2	81.8	66.8
700	183.8	82.1	62.9

geometry and the longer O2—O1 bond length (1.43 Å) and hence weaker bonding (WBI of 1.01) compared to those in the EQ10 (bond length of 1.39 Å and WBI of 1.05). The interconversion between the EQ9 and EQ10 could easily occur via a TS, TS[9-10], because of the low energy barrier (6.7 kcal/mol relevant to the EQ10). As for the bare (HO)<sub>2</sub>PS<sub>2</sub>Cu (Figure 1), the bond-rearrangement isomerization of the EQ10 complex is also a kinetically feasible process leading to an O(H)

bridging structure EQ11. Such an isomerization is an endothermic process (endothermic by 11.1 kcal/mol relevant to the EQ10) and needs to overcome a TS, TS[10-11], with an energy barrier of 12.7 kcal/mol (Figure 2). An analysis of the imaginary vibration mode of the TS[10-11] suggests that the conversion of the EQ10 to EQ11 is achieved by the rotation of the (OH)<sub>2</sub>P1S2 group around the P1—S1 bond axis. Such situation is similar to that of the transformation from EQ0 to EQ2 (Figure 1).

As shown in Figure 2, the EQ9 may serve as a precursor for the (HO)<sub>2</sub>PS<sub>2</sub>Cu-assisted CH<sub>3</sub>OO• decomposition via the cleavage of O1—O2 or C1—O1 bond. The O1—O2 bond cleavage of the EQ9 occurs via TS[9-12] leading to EQ12. The energy barrier for such a process is 24.3 kcal/mol. The O1...O2 distance of 2.71 Å in the EQ12 is rather longer than the sum of the covalent radii of two O atoms (0.73 + 0.73 Å), suggesting no covalent interaction between O1 and O2 in the EQ12. The WBI of ~1.0 for the O1—O2 bond in the EQ9 decreased to be ~0.1 in the EQ12. These results indicate that the O1—O2 bond is dissociated in the EQ12. As shown in Figure 2, another (HO)<sub>2</sub>PS<sub>2</sub>Cu-assisted dissociation process (via the cleavage of the C1—O1 bond) of CH<sub>3</sub>OO• moiety takes place through a direct dissociation channel leading to (HO)<sub>2</sub>PS<sub>2</sub>Cu-(μ,η<sup>2</sup>-)O<sub>2</sub> and •CH<sub>3</sub>. The triplet energy of the dissociated species (HO)<sub>2</sub>PS<sub>2</sub>Cu-(μ,η<sup>2</sup>-)O<sub>2</sub> is lower than its singlet energy by 11.2 kcal/mol at the level of B3LYP/BSII/B3LYP/BSI. Therefore, the triplet energy of this species was used to calculate the dissociation energy (containing basis-set superposition error correction), and the structure of this species shown in Figure 2 is its triplet geometry. Such decomposition reaction requires an energy of 45.9 kcal/mol relevant to the EQ9 (see Figure 2), which is higher than the energy barrier for the conversion of EQ9 to EQ12.

To see the temperature effect on the reactions shown in Figure 2, the relative free energies at various temperatures were also calculated for the stationary points. The results are shown in Table 5. As seen from this table, except for the DC corresponding to the dissociated species (Figure 2) and the reactant species [(HO)<sub>2</sub>PS<sub>2</sub>Cu + CH<sub>3</sub>OO•], the relative free energy slightly increases with temperature. However, the variations are less than 4 kcal/mol. As for the DC, the relative free energy decreases by 15.2 kcal/mol when temperature varies from 300 to 700 K. Such different trends in the relative free energy is due to the two separated species [•CH<sub>3</sub> and (HO)<sub>2</sub>PS<sub>2</sub>Cu-(μ,η<sup>2</sup>-)O<sub>2</sub>] in

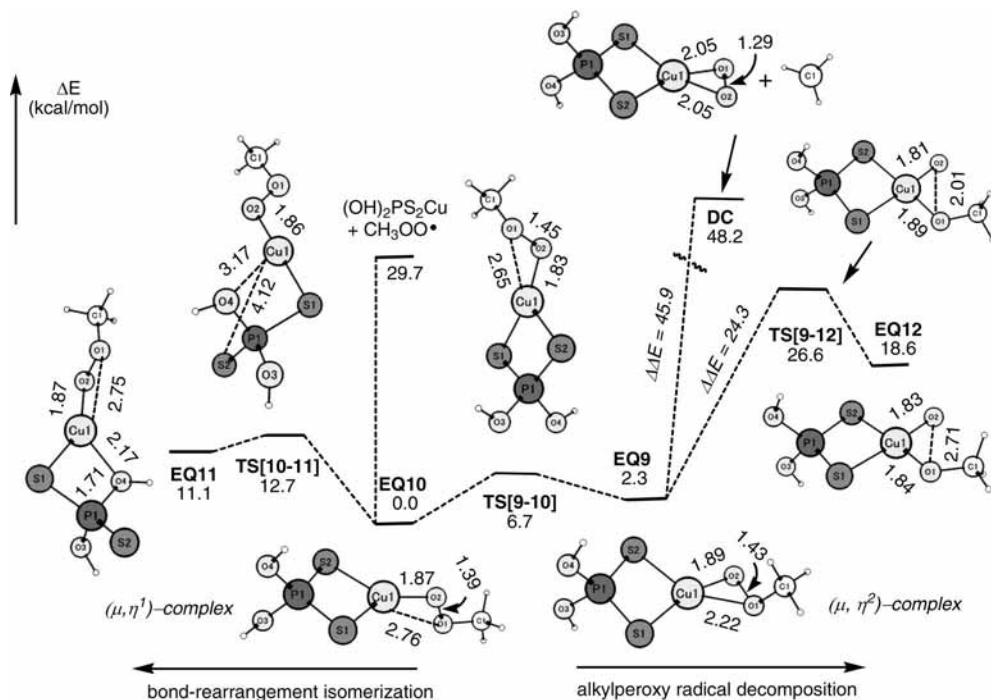


**Figure 2.** Stationary points (bond lengths in angstrom) together with their relative energies (kcal/mol) for the reaction of  $(\text{OH})_2\text{PS}_2\text{Cu}$  with  $\text{CH}_3\text{OO}\cdot$ . The energies computed at the level B3LYP/BSII//B3LYP/BSI are relative to **EQ10**.

**TABLE 5: Temperature Effects on the Relative Free Energies (kcal/mol) of the Stationary Points<sup>a</sup>**

	relative free energies				
	300 (K)	400 (K)	500 (K)	600 (K)	700 (K)
<b>EQ10</b>	0.0	0.0	0.0	0.0	0.0
<b>EQ9</b>	3.6	4.0	4.5	4.9	5.3
<b>EQ11</b>	12.5	12.6	12.8	12.9	13.1
<b>EQ12</b>	19.5	20.0	20.6	21.1	21.6
<b>DC</b>	33.6	29.8	26.0	22.2	18.4
$(\text{OH})_2\text{PS}_2\text{Cu} + \text{CH}_3\text{OO}\cdot$	18.7	15.5	12.3	9.3	6.3
<b>TS[9-10]</b>	7.5	8.0	8.5	9.1	9.8
<b>TS[10-11]</b>	12.4	12.9	13.4	14.0	14.6
<b>TS[9-12]</b>	27.5	28.2	29.0	29.9	30.7

<sup>a</sup> Energies are relative to **EQ10**. The structures of the stationary points are shown in Figure 2.

the **DC**, which is entropically different from other EQs and TSs. This result suggests that a higher temperature is beneficial for this dissociation reaction via the C1–O1 bond cleavage. It is noteworthy that the relative free energy of the **DC** is lower at high temperature (>500 K) but higher at low temperature than that of **TS[9-12]** (Table 5). This result indicates that the dissociation reaction via the C1–O1 bond cleavage is energetically preferable over the conversion of **EQ9** to **EQ12** at such high temperature (>500 K), and the reverse preference is suggested for the formation of the **EQ12** at lower temperature. Like the **DC**, the free energies at various temperatures indicate that the reactant species  $[(\text{OH})_2\text{PS}_2\text{Cu} + \text{CH}_3\text{OO}\cdot]$  get more stable with increasing temperature because of the bimolecular character (Table 5).

In view of the energy profile shown in Figure 2, the conversion of **EQ10** to **EQ9** could occur. Actually, a Boltzmann distribution analysis shows that the **EQ10** predominates and that the **EQ9** has significant population at high temperature. For example, the **EQ9** occupies a population of more than 10% at ~500 K (see Supporting Information). This result suggests that the **EQ9** may coexist with the **EQ10**. It is therefore possible to form **EQ12** and **DC**, both of which may further undergo chemical reactions. The processes shown in Figure 2, such as

**TABLE 6: Solvation Effect<sup>a</sup> on the Relative Free Energies of the Stationary Points Involved in the Reaction of  $(\text{OH})_2\text{PS}_2\text{Cu}$  With  $\text{CH}_3\text{OO}\cdot$**

relative energy, (kcal/mol)	TS		TS		TS		
	<b>EQ10</b>	<b>[10-11]</b>	<b>EQ11</b>	<b>[9-10]</b>	<b>EQ9</b>	<b>[9-12]</b>	<b>EQ12</b>
$\Delta G(\text{gas})$	0.0	12.4	12.5	7.4	3.2	27.5	19.5
$\Delta G(\text{sol})$	0.0	12.0	11.8	6.0	2.3	25.7	17.6

<sup>a</sup> The solvation free energy calculations were based on the gas-phase optimized geometries. The CPCM model was used, and heptane was selected as a solvent. The Gibbs free energy contributions from the gas-phase calculations were added to give the final solvation free energies,  $\Delta G(\text{sol})$  (298 K, 1 atm.).

the formation of the **EQ9** and its conversion to the **EQ12** and **DC**, may be relevant to the reaction of CuDDP with alkylperoxy radicals.

As a result of automatic search for the pathways by the SHS method, an additional dissociation channel of the **EQ9** was also found, which led to  $\cdot\text{OH}$  and  $\text{HO}(\cdot\text{P})\text{S}_2\text{Cu}-(\mu,\eta^2)\text{-OOCH}_3$  via cleavage of a P–O bond. It needs a high energy (more than 70 kcal/mol) under the investigated conditions and is unlikely to occur. Such a dissociation reaction, which is not shown in Figure 2, is similar to that for the bare  $(\text{HO})_2\text{PS}_2\text{Cu}$  compound. The bare  $(\text{HO})_2\text{PS}_2\text{Cu}$  compound also shows a high dissociation energy (63 ~79 kcal/mol) for the P–O bond cleavage leading to  $\cdot\text{OH}$  and  $\text{HO}(\cdot\text{P})\text{S}_2\text{Cu}$  (Table 4). This result suggests that the  $(\text{HO})_2\text{PS}_2\text{Cu}$ -assisted decomposition of  $\text{CH}_3\text{OO}\cdot$  could occur prior to the self-decomposition of  $(\text{HO})_2\text{PS}_2\text{Cu}$ , which may account for the antioxidation behavior of CuDDP.

Considering the fact that CuDDP as an antioxidant is added to the base stock, which mainly consists of alkanes, the solvation effect on the energies was also estimated for the reaction of  $(\text{HO})_2\text{PS}_2\text{Cu}$  with  $\text{CH}_3\text{OO}\cdot$ . The relative solvation free energies of some stationary points (Figure 2) are given in Table 6. For comparison, the relative free energies in gas phase are also included in this table. It is found that the solvation slightly decreases these energies (by less than 2 kcal/mol) because of

the nonpolarity of such alkane solvent. This suggests that such reactions may not be much energetically affected by the solvation.

## Conclusion

A computational study has been performed for the isomerization and decomposition of  $(\text{OH})_2\text{PS}_2\text{Cu}$ , as a model compound of cuprous dialkyldithiophosphate and its reaction with  $\text{CH}_3\text{OO}\cdot$ . The SHS method developed by our group has been utilized for exploring the reaction PES. Among the structures of  $(\text{OH})_2\text{PS}_2\text{Cu}$ , which are found in this study, the isomer having four-membered ring (PSCuS) was computed to be the most stable. Such a structural form is in line with an experimental structure of its derivatives. It has been found that the isomerization of  $(\text{OH})_2\text{PS}_2\text{Cu}$  involves various chemical bond rearrangements, such as the  $(\text{H})\text{O}-\text{Cu}$  bond formation concerted with a  $\text{S}-\text{Cu}$  bond cleavage leading to an  $(\text{H})\text{O}$ -bridging structure. Such bond-rearrangement isomerizations are kinetically feasible but endothermic. Three dissociation channels have also been found for the  $(\text{OH})_2\text{PS}_2\text{Cu}$ . These dissociation reactions of  $(\text{OH})_2\text{PS}_2\text{Cu}$  require rather high energies and could not energetically compete against its isomerization processes. The reaction of  $(\text{OH})_2\text{PS}_2\text{Cu}$  with  $\text{CH}_3\text{OO}\cdot$  may undergo bond-rearrangement isomerization. The  $(\text{OH})_2\text{PS}_2\text{Cu}$ -assisted  $\text{O}-\text{O}$  bond cleavage of  $\text{CH}_3\text{OO}\cdot$  is endothermic but feasible because of a moderate energy barrier. The  $(\text{OH})_2\text{PS}_2\text{Cu}$ -assisted  $\text{CH}_3\text{OO}\cdot$  dissociation via its  $\text{C}-\text{O}$  bond dissociation is favorable at the high temperature ( $>500$  K) investigated compared to the  $\text{O}-\text{O}$  bond cleavage process. The replacement of H with alkyl group R and the alkane solvation have been computationally found to not significantly affect the energetic aspect of the selected reactions. However, a higher temperature may accelerate some dissociation reactions. Further studies on the CuDDP-involved reactions in lubricating oil are in progress.

**Acknowledgment.** Y.L. acknowledges Japan Society for the Promotion of Science (JSPS) for research fellowship. S.M. is supported by JSPS for Young Scientists.

**Supporting Information Available:** Figures and tables giving the optimized structures of  $(\text{HO})_2\text{PS}_2\text{Cu}$  at various computational levels, the Boltzmann distribution of the **EQ9** and **EQ10**, and the optimized Cartesian coordinates of the stationary points. This material is available free of charge via the Internet at <http://pubs.acs.org>.

## References and Notes

- (1) For reviews, see: (a) Hironaka, S. *J. Jpn. Soc. Tribol.* **1997**, *42*, 169–174. (b) Barnes, A. M.; Bartle, K. D.; Thibon, V. R. *Tribol. Int.* **2001**, *34*, 389–395. (c) Waynick, J. A. *Energy Fuels* **2001**, *15*, 1325–1340. (d) Spikes, H. *Tribol. Lett.* **2004**, *17*, 469–489.
- (2) Reich, L.; Stivala, S. S. *Autoxidation of hydrocarbons and Polyolefins*; Marcel Dekker: New York, 1969.
- (3) Mcnab, J. G.; Hakala, N. V.; Mcdermott, J. P. Patent no. US 2,552,570, 1951.
- (4) (a) Zhang, Z. F.; Liu, W. M.; Xue, Q. *J. Analyst* **1992**, *117*, 207–210. (b) Luo, Y.; Ran, X. *Speciality Petrochemicals* **1998**, *6*, 37–39.
- (5) Hunt, W.; Kennedy, S. Patent no. US 4,664,822-A, AU 8,665,531-A, 1987; US 4767551-A, 1988.
- (6) Frosschman, E. Patent no. EP 2,86,139-A, WO 8,808,021-A, 1988; JP 1,503,543-W, 1989.
- (7) Hata, H. Patent no. US 5,133,886-A, 1992; EP 475,141, 1994; JP 2,923,341-B1, 1999.
- (8) Stemmler, K.; Gunten, U. V. *Atmos. Environ.* **2000**, *34*, 4253–4264.
- (9) Tripathi, U. N.; Bohra, R.; Srivastava, B. G.; Mehrotra, R. C. *Polyhedron* **1992**, *11*, 1187–1194.
- (10) Liu, C. W.; Irwin, M. D.; Mohamed, A. A.; Fackler, J. P. *Inorg. Chim. Acta* **2004**, *357*, 3950–3956.
- (11) Liaw, B. J.; Lobana, T. S.; Lin, Y. W.; Wang, J. C.; Liu, C. W. *Inorg. Chem.* **2005**, *44*, 9921–9929.
- (12) Li, Z. H.; Li, J. R.; Du, S. W. *J. Mol. Struct.* **2006**, *783*, 116–121.
- (13) (a) Rusanova, D.; Pike, K. J.; Persson, I.; Hanna, J. V.; Dupree, R.; Forsling, W.; Antzutkin, O. N. *Chem. Eur. J.* **2006**, *12*, 5282–5292. (b) Rusanova, D.; Pike, K. J.; Dupree, R.; Hanna, J. V.; Antzutkin, O. N.; Persson, I.; Forsling, W. *Inorg. Chim. Acta* **2006**, *359*, 3903–3910. (c) Rusanova, D.; Christensen, K. E.; Persson, I.; Pike, K. J.; Antzutkin, O. N.; Zou, X.; Dupree, R.; Forsling, W. *J. Coord. Chem.* **2007**, *60*, 517–525.
- (14) Mosey, N. J.; Woo, T. K. *J. Phys. Chem. A* **2003**, *107*, 5058–5070; *J. Phys. Chem. A* **2004**, *108*, 6001–6016; *Inorg. Chem.* **2005**, *44*, 7274–7276; *Tribol. Int.* **2006**, *39*, 979–993.
- (15) (a) Ohno, K.; Maeda, S. *Chem. Phys. Lett.* **2004**, *384*, 277–282. (b) Maeda, S.; Ohno, K. *J. Phys. Chem. A* **2005**, *109*, 5742–5753. (c) Ohno, K.; Maeda, S. *J. Phys. Chem. A* **2006**, *110*, 8933–8941.
- (16) (a) Yang, X.; Maeda, S.; Ohno, K. *J. Phys. Chem. A* **2005**, *109*, 7319–7328. (b) Yang, X.; Maeda, S.; Ohno, K. *Chem. Phys. Lett.* **2006**, *418*, 208–216. (c) Yang, X.; Maeda, S.; Ohno, K. *J. Phys. Chem. A* **2007**, *111*, 5099–5110. (d) Watanabe, Y.; Maeda, S.; Ohno, K. *Chem. Phys. Lett.* **2007**, *447*, 21–26.
- (17) (a) Luo, Y.; Maeda, S.; Ohno, K. *J. Phys. Chem. A* **2007**, *111*, 10732–10737. (b) Maeda, S.; Ohno, K. *J. Phys. Chem. A* **2007**, *111*, 4527–4534. (c) Maeda, S.; Ohno, K. *J. Phys. Chem. A* **2008**, *112*, 2962–2968.
- (18) (a) Svensson, M.; Humbel, S.; Froese, R. D. J.; Matsubara, T.; Sieber, S.; Morokuma, K. *J. Phys. Chem.* **1996**, *100*, 19357–19363. (b) Dapprich, S.; Komromi, I.; Byun, K. S.; Morokuma, K.; Frisch, M. J. *J. Mol. Struct. (theochem)* **1999**, *461–462*, 1–21. (c) Vreven, T.; Morokuma, K. *J. Comput. Chem.* **2000**, *21*, 1419–1432. (d) Vreven, T.; Morokuma, K.; Farkas, Ö.; Schlegel, H. B.; Frisch, M. J. *J. Comput. Chem.* **2003**, *24*, 760–769.
- (19) Maeda, S.; Ohno, K. *J. Phys. Chem. A* **2007**, *111*, 13168–13171.
- (20) (a) Lee, C.; Yang, W.; Parr, R. G. *Phys. Rev.* **1988**, *B37*, 785–789. (b) Backe, D. *J. Chem. Phys.* **1993**, *98*, 5648–5652.
- (21) (a) Hay, P. J.; Wadt, W. R. *J. Chem. Phys.* **1985**, *82*, 270–283. (b) Hay, P. J.; Wadt, W. R. *J. Chem. Phys.* **1985**, *82*, 299–310.
- (22) (a) Petersson, G. A.; Al-Laham, M. A. *J. Chem. Phys.* **1991**, *94*, 6081–6090. (b) Petersson, G. A.; Bennett, A.; Tensfeldt, T. G.; Al-Laham, M. A.; Shirley, W. A.; Mantzaris, J. *J. Chem. Phys.* **1988**, *89*, 2193–2218. (c) Clark, T.; Chandrasekhar, J.; Spitznagel, G. W.; Schleyer, P. R. *J. Comput. Chem.* **1983**, *4*, 294–301.
- (23) Hollwarth, A.; Bohme, M.; Dapprich, S.; Ehlers, A. W.; Gobbi, A.; Jonas, V.; Kohler, K. F.; Veldkamp, R.; Frenking, G. *Chem. Phys. Lett.* **1993**, *208*, 111–114.
- (24) (a) Wachters, A. J. H. *J. Chem. Phys.* **1970**, *52*, 1033–1036. (b) Hay, P. J. *J. Chem. Phys.* **1977**, *66*, 4377–4384.
- (25) (a) Krishnan, R.; Binkley, J. S.; Seeger, R.; Pople, J. A. *J. Chem. Phys.* **1980**, *72*, 650–654. (b) McLean, A. D.; Chandler, G. S. *J. Chem. Phys.* **1980**, *72*, 5639–5648.
- (26) Frisch, M. J.; Trucks, G. W.; Schlegel, H. B.; Scuseria, G. E.; Robb, M. A.; Cheeseman, J. R.; Montgomery, J. A., Jr.; Vreven, T.; Kudin, K. N.; Burant, J. C.; Millam, J. M.; Iyengar, S. S.; Tomasi, J.; Barone, V.; Mennucci, B.; Cossi, M.; Scalmani, G.; Rega, N.; Petersson, G. A.; Nakatsuji, H.; Hada, M.; Ehara, M.; Toyota, K.; Fukuda, R.; Hasegawa, J.; Ishida, M.; Nakajima, T.; Honda, Y.; Kitao, O.; Nakai, H.; Klene, M.; Li, X.; Knox, J. E.; Hratchian, H. P.; Cross, J. B.; Bakken, V.; Adamo, C.; Jaramillo, J.; Gomperts, R.; Stratmann, R. E.; Yazyev, O.; Austin, A. J.; Cammi, R.; Pomelli, C.; Ochterski, J. W.; Ayala, P. Y.; Morokuma, K.; Voth, G. A.; Salvador, P.; Dannenberg, J. J.; Zakrzewski, V. G.; Dapprich, S.; Daniels, A. D.; Strain, M. C.; Farkas, O.; Malick, D. K.; Rabuck, A. D.; Raghavachari, K.; Foresman, J. B.; Ortiz, J. V.; Cui, Q.; Baboul, A. G.; Clifford, S.; Cioslowski, J.; Stefanov, B. B.; Liu, G.; Liashenko, A.; Piskorz, P.; Komaromi, I.; Martin, R. L.; Fox, D. J.; Keith, T.; Al-Laham, M. A.; Peng, C. Y.; Nanayakkara, A.; Challacombe, M.; Gill, P. M. W.; Johnson, B.; Chen, W.; Wong, M. W.; Gonzalez, C.; Pople, J. A. *Gaussian 03*, revision D.02; Gaussian, Inc.: Wallingford, CT, 2004.
- (27) (a) Head-Gordon, M.; Pople, J. A.; Frisch, M. J. *Chem. Phys. Lett.* **1988**, *153*, 503–506. (b) Saebo, S.; Almlof, J. *Chem. Phys. Lett.* **1989**, *154*, 83–89. (c) Frisch, M. J.; Head-Gordon, M.; Pople, J. A. *Chem. Phys. Lett.* **1990**, *166*, 275–280. (d) Frisch, M. J.; Head-Gordon, M.; Pople, J. A. *Chem. Phys. Lett.* **1990**, *166*, 281–289. (e) Head-Gordon, M.; Head-Gordon, T. *Chem. Phys. Lett.* **1994**, *220*, 122–128.